

Figure S1: <sup>1</sup>H NMR spectra in DMSO-d<sub>6</sub> of (a) pure 3-TPT and 3-TPT mixed with CsPbI<sub>2</sub>Br, and (b) pure 4-TPT and 4-TPT mixed with CsPbI<sub>2</sub>Br.

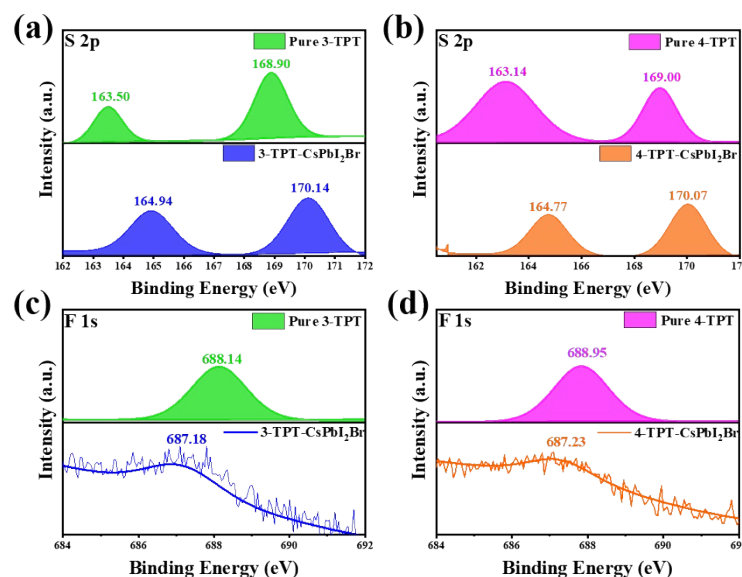


Figure S2: XPS S 2p spectra of (a) pure 3-TPT and 3-TPT-CsPbI<sub>2</sub>Br, and (b) pure 4-TPT and CsPbI<sub>2</sub>Br; XPS F 1s spectra of (c) pure 3-TPT and 3-TPT-CsPbI<sub>2</sub>Br, and (d) pure 4-TPT and 4-TPT-CsPbI<sub>2</sub>Br.

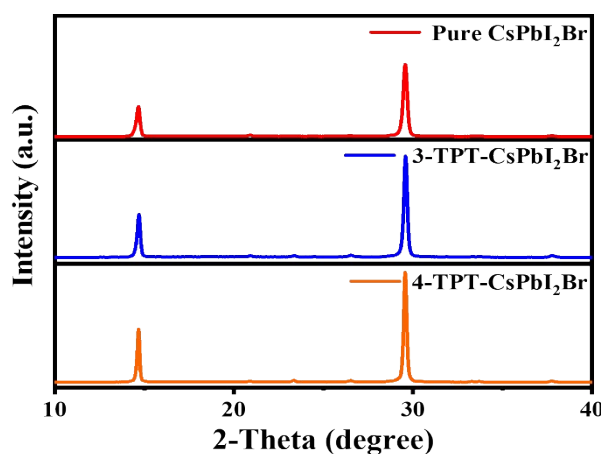


Figure S3: XRD patterns for pure CsPbI<sub>2</sub>Br, 3-TPT-CsPbI<sub>2</sub>Br, and 4-TPT-CsPbI<sub>2</sub>Br.

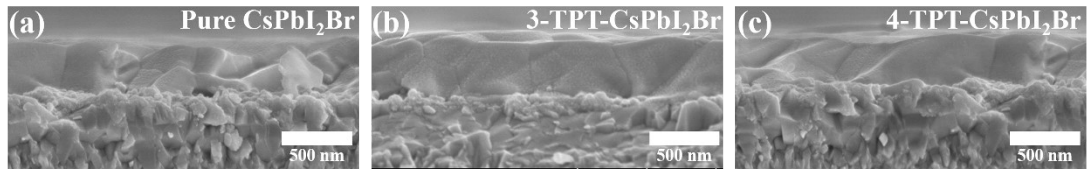


Figure S4: Cross-sectional SEM images of (a)  $\text{CsPbI}_2\text{Br}$ , (b) 3-TPT- $\text{CsPbI}_2\text{Br}$ , and (c) 4-TPT- $\text{CsPbI}_2\text{Br}$ .

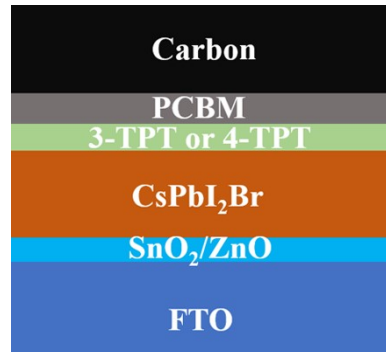


Figure S5: Schematic representation of the structure of carbon-based  $\text{CsPbI}_2\text{Br}$  devices ( $\text{FTO}/\text{SnO}_2/\text{ZnO}/\text{CsPbI}_2\text{Br}/$  3-TPT or 4-TPT/PCBM/ carbon) for SCLC.

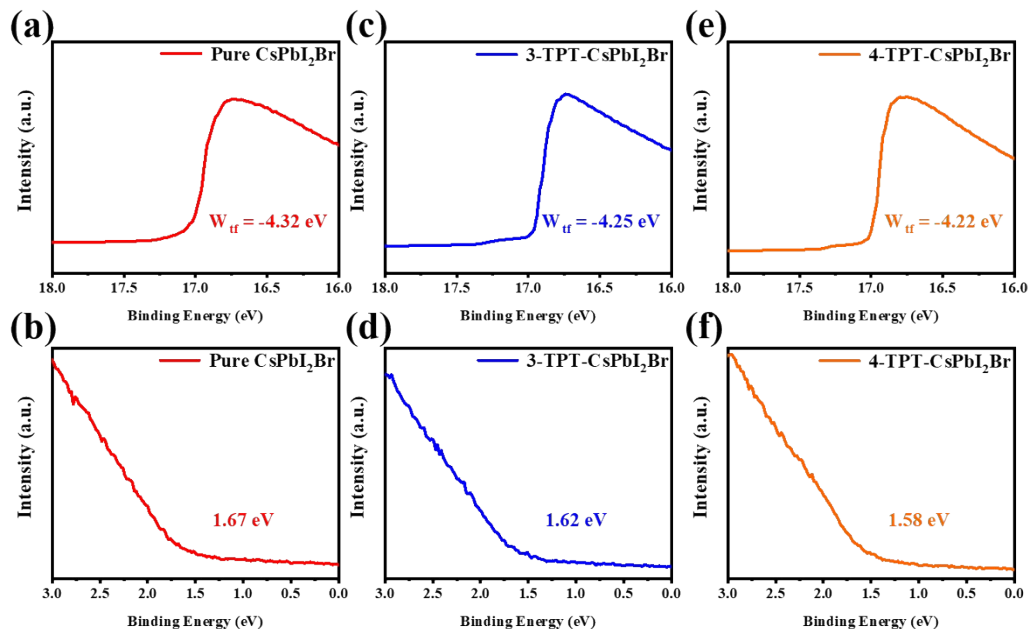


Figure S6: Ultraviolet photoelectron spectroscopic (UPS) analysis of (a) pure  $\text{CsPbI}_2\text{Br}$ , (b) 3-TPT- $\text{CsPbI}_2\text{Br}$ , and (c) 4-TPT- $\text{CsPbI}_2\text{Br}$ .

Table S1. The optical properties of  $\text{CsPbI}_2\text{Br}$ , 3-TPT- $\text{CsPbI}_2\text{Br}$  and 4-TPT- $\text{CsPbI}_2\text{Br}$  by UPS characterization.

Sample	$E_{\text{cut-off}}$ (eV)	$E_V - E_F$ (eV)	$E_F$ (eV)	$E_V$ (eV)	$E_C$ (eV)	$E_g$ (eV)
Pure $\text{CsPbI}_2\text{Br}$	16.90	1.67	4.32	5.99	4.07	1.92
3-TPT- $\text{CsPbI}_2\text{Br}$	16.97	1.62	4.25	5.87	3.95	1.92
4-TPT- $\text{CsPbI}_2\text{Br}$	17.02	1.58	4.20	5.78	3.86	1.92

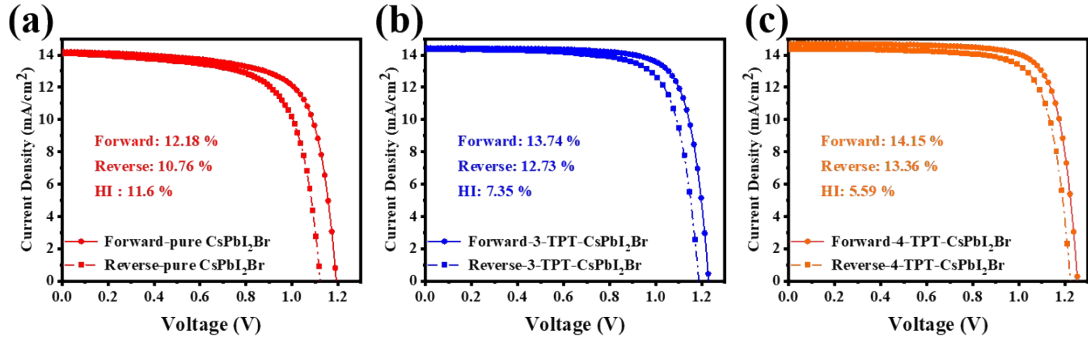


Figure S7: The J-V curves for pure CsPbI<sub>2</sub>Br, 3-TPT-CsPbI<sub>2</sub>Br, and 4-TPT-CsPbI<sub>2</sub>Br devices in both forward and reverse scans.

Table S2. Performance parameters of pure CsPbI<sub>2</sub>Br, 3-TPT-CsPbI<sub>2</sub>Br, and 4-TPT-CsPbI<sub>2</sub>Br devices in both forward and reverse scans, derived from J-V curves.

Sample	V <sub>oc</sub> (V)	J <sub>sc</sub> (mA/cm <sup>2</sup> )	Fill factor	PCE (%)	HI (%)
Forward-Pure CsPbI <sub>2</sub> Br	1.19	14.19	72.14	12.18	11.66
Reverse-Pure CsPbI <sub>2</sub> Br	1.12	14.10	68.12	10.76	
Forward-3-TPT-CsPbI <sub>2</sub> Br	1.23	14.42	77.47	13.74	7.35
Reverse-3-TPT-CsPbI <sub>2</sub> Br	1.19	14.37	74.48	12.73	
Forward-4-TPT-CsPbI <sub>2</sub> Br	1.25	14.47	78.22	14.15	5.59
Reverse-4-TPT-CsPbI <sub>2</sub> Br	1.22	14.39	76.25	13.39	

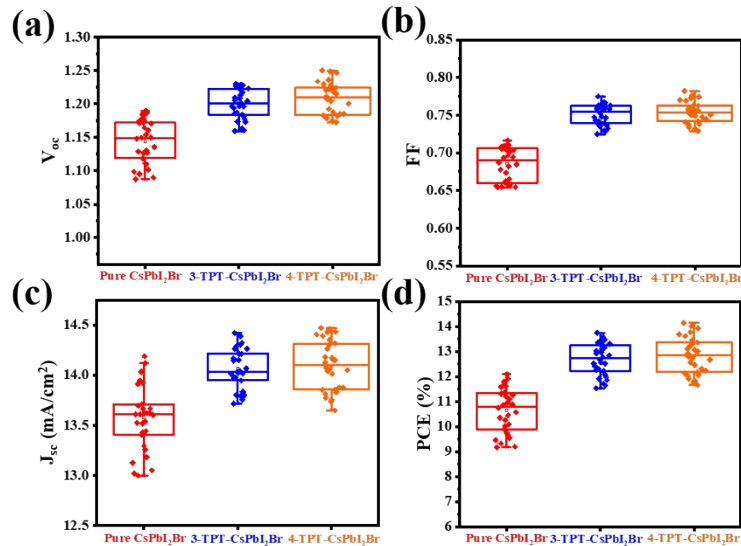


Figure S8: Boxplot distributions for 30 solar cell devices based on pure CsPbI<sub>2</sub>Br, 3-TPT-CsPbI<sub>2</sub>Br, and 4-TPT-CsPbI<sub>2</sub>Br, illustrating (a) V<sub>oc</sub>, (b) FF, (c) J<sub>sc</sub>, and (d) PCE.